Nanocarriers for Biomedical Applications

Shuyi Li[a], Lynsa Nguyen[b], Hairong Xiong[a,c], Meiyao Wang[d], Tom C.-C. Hu[b], Jin-Xiong She[d], Steven M. Serkiz[e], George G. Wicks[e], and William S. Dynan*[a]

**Corresponding author. Tel:706-721-8756; E-mail: wdynan@georgiahealth.edu.*
[a]Institute of Molecular Medicine and Genetics, Georgia Health Sciences University, Augusta, GA 30912
[b]Small Animal Imaging, Department of Radiology, , Georgia Health Sciences University, Augusta, GA 30912
[c]Institute of Medical Virology, Wuhan University, Hubei Province, China 430071
[d]Center for Biotechnology and Genomic Medicine, , Georgia Health Sciences University, Augusta, GA 30912
[e]Savannah River National Laboratory, Aiken, South Carolina 29808

Porous-wall hollow glass microspheres (PW-HGMs) show promise for drug delivery applications. They are a novel ceramic biocompatible material with a hollow central cavity surrounded by a thin mesoporous shell. The central cavity can be loaded with a high concentration of a soluble biological therapeutic, for example a small RNA, protein, or antibody fragment. The thin silica shell protects the contents from environmental conditions. Nanometer-scale channels penetrate the shell, providing for controlled uptake and release of the protected material from the central cavity. We have developed a gating strategy that potentially allows the pores to be opened and closed. The hollow interior, protective walls, and gated, controlled-porosity channels distinguish the technology from competing drug delivery approaches.

Introduction

Conventional drug delivery relies on oral ingestion or injection. These methods do not allow delivery to specific anatomic sites. In addition, macromolecular drugs (peptides, proteins, antibodies, DNA, and RNA) are often poor candidates for delivery by these routes due to their instability, limited tissue penetration, or rapid turnover. The global drug market has witnessed a significant growth in development of macromolecular drugs, yet delivery remains a limiting factor.

Bioactive glass materials, or composites of bioactive glass and polymers, have shown promise as carriers for both small molecules and protein therapeutics, such as vascular endothelial growth factor and bone morphogenetic proteins [1-5]. Glass materials have also been developed as a therapeutic radiation delivery system [6-8].

Currently, use of glass materials for delivery of therapeutic agents requires either bonding to organic polymers or the deposition of chemical substances directly into the glass matrix. We recently described a more general approach for drug delivery using glass materials [9]. The approach is based on porous-wall hollow glass microspheres (PW-HGMs), which are micron-scale glass "balloons" with an internal cavity bounded by a 1 µm-thick mesoporous wall [10]. PW-HGMs are generally fabricated in sizes ranging from 10 to 100 µm. The hollow central cavity can be loaded with a high concentration of a soluble biological therapeutic, for example a small RNA, protein, or antibody fragment. In addition, the walls are characterized by worm-like, interconnected channels in a silica-rich matrix [10]. Together, these characteristics allow them to function as carriers for diverse materials.

We hypothesized that PW-HGMs might be useful for controlled delivery of macromolecular therapeutics. We therefore tested their ability to interact with proteins, carbohydrates, and nucleic acids [12] In this chapter, we summarize the results of our studies. These results suggest that PW-HGMs may be useful as a controlled release delivery vehicle for both protein and oligonucleotide therapeutics.

Materials and Methods

Fabrication of PW-HGMs

Details of the process have been described elsewhere, along with methodologies for loading or filling these materials [11-14]. Briefly, the feed for producing PW-HGMs was a 20-40 µm sodium borosilicate glass powder, similar to commercial Vycor, and containing a sulfate blowing agent. The powder was fed into a hot zone produced by a controlled gas-air flame, which softens the glass to allow formation of spherical particles. The material was quenched, and a flotation process was used to retrieve the desired initial products. These were heat-treated to produce two phases in the thin outer walls, one rich in silica and the other in sodium and boron. The hollow microspheres were treated with 4 M HCl, which preferentially leaches the sodium and boron-rich phase, leaving interconnected channels in the silica-rich phase.

Fluorescently-labeled biopolymers

Fluorescein-labeled dextrans were obtained from Sigma-Aldrich (St. Louis, MO). A 55 base pair 5'-Alex Fluor 546-labeled oligonucleotide was prepared as described [9]. Cy 3-labeled GAPDH siRNA was from Applied Biosystems (Austin, TX). Alexa Fluor 594-labeled goat anti-rabbit IgG was obtained from Invitrogen.

Biopolymer loading

Dry PW-HGMs (2-3 mg) were suspended in 50-100 µl of PBS containing 200 µg/ml of biopolymer and incubated at room temperature for 5-10 min. A portion was used for direct observation, and the remainder was collected by gentle centrifugation, washed with 0.5 ml of PBS or fetal bovine serum, and centrifuged again. The pellet was resuspended in 50-100 µl of PBS or fetal bovine serum for imaging. Microscopy was performed using a Zeiss LSM 510 laser

scanning confocal microscope with a 40X or a 63X oil objective or an Applied Precision Deltavision microscope with a 20X or a 60X oil objective.

Mouse imaging

Animal experiments were performed at the Medical College of Georgia according to an Institutional Animal Care and Use Committee-approved protocol. PW-HGMs (3.3 mg) were incubated with fluorescein-labeled 70 kDa dextran (200 µg/ml) in 100 µl PBS. Just before use, PW-HGMs were washed twice with PBS and resuspended in 500 µL of PBS. Fluorescence images were collected using a Xenogen IVIS Imaging System equipped with 445-490 nm bandpass filter for excitation and a 515-575 nm bandpass filter for emissions. Images were acquired with a 1 s exposure, and LivingImage 2.60 Software was used to perform a fluorescent overlay, which allowed the subtraction of background to produce the final images.

Results and Discussion

Interaction of PW-HGMs with biological macromolecules

The diameters of PW-HGMs ranged from 10 to 100 µm. with a typical wall thickness of 1 µm (Fig. 1A). Scanning electron microscopy (not shown, see ref. [9]) reveals the presence of ink-bottle shaped pores in the outer shell, with diameters ranging from about 10 nm, at the narrowest point, to about 300 nm. These pores, which connect the exterior space with the interior volume of the microspheres, are the distinguishing characteristic of PW-HGMs.

To investigate the ability of biological polymers to penetrate the interior volume of the PW-HGMs, we performed experiments using fluorescently-labeled dextrans, proteins, and nucleic acids. A 500 kDa dextran, with an estimated diameter of about 14.4 nm, failed to enter the microspheres (Fig. 1B), whereas a smaller, 70 kDa dextran, with an estimated diameter of 6.0 nm, freely equilibrated with the interior volume. Results with these and other dextrans [9] suggest that the porous walls behave as molecular sieves, passing the smaller dextrans and excluding the larger.

Interestingly, the 70 kDa dextran accumulated in the microsphere walls to levels exceeding its concentration in solution, a behavior not seen with any of the larger or smaller dextrans (Fig. 1B and data not shown, see ref [9]). The 70 kDa dextran is about the same size as the diameter of the pores themselves, and we hypothesize that it is of a critical size that allows a large fraction of its surface area to contact the wall material at any given time, stabilizing its interaction.

A fluorescently-labeled Immunoglobulin G (IgG), which is about the same size as the 70 kDa dextran (5.3 nm) behaved similarly, with concentration and retention in the microsphere walls. By contrast, several smaller proteins, including ovalbumin, carbonic anhydrase, and RNase A, entered the PW-HGMs freely but showed little retention after washing (data not shown, see ref [9]). We suggest that they are too small to make a sufficient number of contacts with the walls of the pores, accounting for poor retention.

We also explored the interactions of PW-HGMs with nucleic acids. A double-stranded 55-mer DNA behaved much like the smaller dextrans and proteins, freely entering and exiting the interior volume, with some retention within the porous walls after washing (data not shown, see ref [9]). A double-stranded 21-mer small interfering RNA (siRNA) behaved similarly to the DNA, freely equilibrating between the exterior medium and the interior cavity (Fig. 1B).

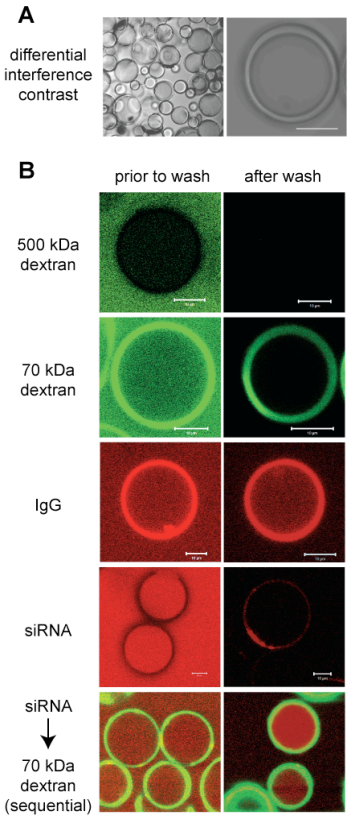

Fig.1 Interaction of PW-HGMs with biological macromolecules. A. Single optical sections, differential interference contrast. Low power (left) and high power (right) images are shown. Scale bar at right, 10 µm. B. Single optical sections of PW-HGMs incubated with indicated compounds and imaged prior to washing (left column) or after washing (right column). Bottom panels show sequential incubation with siRNA, then 70 kDa FITC-Dextran. All panels same magnification, scale bar, 10 µm. Note retention of siRNA by FITC-dextran-gated PH-HGMs.

SiRNAs are of particular interest because they are in widespread development as therapeutic agents. Efficient delivery methods are the limiting factor in many applications (reviewed in [15,16]). Based on the idea that the 70 kDa dextran was about the same size as the diameter of the pores, we investigated whether it could be used to "gate" them in order to control the uptake or release of nucleic acid cargo. We loaded the PW-HGMs with red fluorescently-labeled siRNA, then incubated with green fluorescently-labeled 70 kDa dextran. Prior to washing, the RNA was seen inside the PW-HGMs, and the dextran was enriched within the walls (Fig. 1B). After washing, some PW-HGMs retained the siRNA (although it leached out of others) (Fig. 1B). We performed time-lapse studies of release of siRNA from individual PW-HGMs (data not shown, see ref [9]). The signal density for siRNA was bright initially and declined with time. These results suggest that, in principle, PW-HGMs may be useful as a controlled release delivery vehicle for siRNA.

Visualization of PW-HGMs *in vivo*

The PW-HGMs are considerably larger than blood cells and are thus too large for systemic administration by an intravenous route. We envision their use in applications, such as tumor embolization or tissue regeneration, where there is a need to retain the therapeutic molecules at a localized site. In this application, it would be ideal to be able to visualize the initial placement of the PW-HGMs and their retention at the desired site.

As a first step toward determining whether PW-HGMs could

be visualized in vivo, we tested the ability to detect them using a standard small-animal imaging system. We loaded PW-HGMs with fluorescently-labeled 70 kDa dextran, transferred

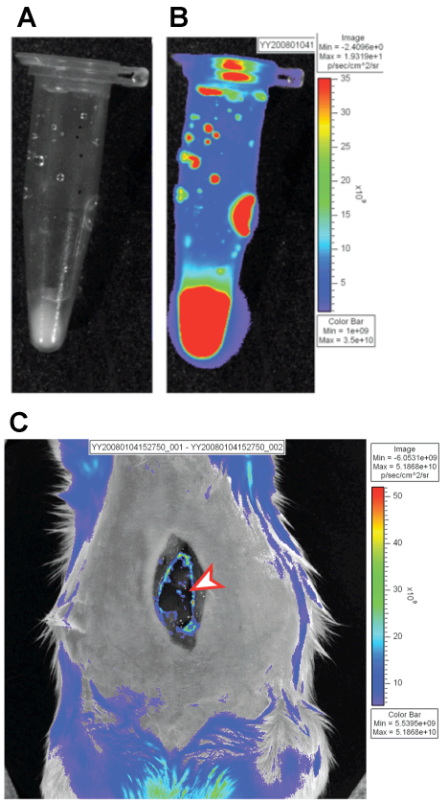

Fig. 2 Beads were incubated with 70 kDa FITC-dextran and washed as in Figure 1. A. White light image. B. Fluorescence image of same tube. C. Visualization in a mouse. Mouse was anesthetized, laparotomized, liver was injected with 10, 30, and 50 µl boluses of beads, and mouse was immediately imaged for green fluorescence. Arrowhead denotes signal at injection site. Note also signal around periphery of liver, possibly following leakage along injection track.

them to microcentrifuge tube, and performed imaging as described in Materials and Methods. The method proved to be very sensitive, as evidenced by the ability to detect even very small droplets of PW-HGM slurry on the walls of the tube (Fig. 2A, 2B). Quantitative image analysis, reported elsewhere, reveals a linear relationship between the amount of material loaded and the corresponding photon counts [9]. We also injected of the same PW-HGMs into the liver of an anesthetized, laparotomized mouse. The image shows clear localization at the site of injection (Fig. 2C), with some signal also around the periphery of the liver, possibly following leakage along the injection track. In experiments elsewhere, we have also shown the ability to detect PW-HGMs *in situ* following intratumoral injection [9].

Conclusions

The results suggest that PW-HGMs may be useful for delivery of macromolecular therapeutics. Interaction of biomolecules is strongly size dependent, and there are several examples of molecules of a critical size that interact strongly with the porous walls. In the case of 70 kDa dextran, we show that this molecule can actually be used to gate the pores, so as to obtain controlled release of a small RNA from the interior volume. We show also that it is possible to visualize the initial placement of PW-HGMs in vivo using standard small animal imaging approaches.

References

1. Leach, J.K., Kaigler, D., Wang, Z., Krebsbach, P.H. and Mooney, D.J. *Biomaterials,* **2006**, *27*, 3249.

2. Bergeron, E. Marquis, M.E., Chretien, I. and Faucheux, N. *J Mater Sci Mater Med,* **2007**, *18*, 255.

3. Xia, W. , Chang, J., Lin, J. and Zhu, J. *Eur J Pharm Biopharm,* **2008**, *69,* 546.

4. Balamurugan, A., Balossier, G., Laurent-Maquin, D., Pina, S., Rebelo, A.H., Faure, J. and Ferreira, J.M. *Dent Mater,* **2008,** *24,* 1343.

5. Friedman, A.J., Han, G., Navati, M.S., Chacko, M., Gunther, L. Alfieri, A. and Friedman, J.M. *Nitric Oxide,* **2008**, *19*, 12.

6. Conzone, S.D., Hall, M.M., Day, D.E. and Brown, R.F. *J Biomed Mater Res A,* **2004**, *70*, 256.

7. Ibrahim, S.M., Lewandowski, R.J., Sato, K.T., Gates, V.L, Kulik, L. Mulcahy, M.F., Ryu, R.K., Omary, R.A. and Salem, R. *World J Gastroenterol,* **2008**, *14*, 1664.

8. Salem, R. and Hunter, R.D. *Int J Radiat Oncol Biol Phys,* **2006,** *66*, S83.

9. Li, S. , Nguyen, L., Xiong, H., Wang, M., Hu, T.C., She, J.X., Serkiz, S.M., Wicks, G.G. and Dynan, W.S. *Nanomedicine,* **2010**, *6*, 127.

10. Wicks, G.G., Heung, L.K. and Schumacher, R.F. *Am Ceram Soc Bull,* **2008,** *87*, 23.

11. Schumacher, R. inventor, patent application number PCT/US2006/046167, **2006.**

12. Schumacher, R., Wicks, G.G. and Heung, L.K. inventor, patent application number 10/946,464, **2004.**

13. Schumacher, R., Wicks, G.G., Heung, L.K., Hansen, E.K. and Peeler, D.K. inventor, patent application number 12/315,544, **2008.**

14. Schumacher, R., Wicks, G.G. and Heung, L.K. inventor, patent application number 11/256,442, **2005.**

15. Kim, D. and Rossi, J. *Biotechniques,* **2008**, *44*, 613.

16. Juliano, R., Alam, M.R., Dixit, V. and Kang, H. *Nucleic Acids Res,* **2008**, *36*, 4158.